Journal of Materials Science & Technology 32 (2016) 162–166

Contents lists available at ScienceDirect

Journal of Materials Science & Technology

journal homepage: www.jmst.org

Shape Memory Effect, Thermal Expansion and Damping Property of Friction Stir Processed NiTip/Al Composite

D.R. Ni [1], J.J. Wang [1,2], Z.Y. Ma [1,*]

[1] Shenyang National Laboratory for Materials Science, Institute of Metal Research, Chinese Academy of Sciences, Shenyang 110016, China
[2] College of Material Science and Engineering, Shenyang Aerospace University, Shenyang 110136, China

ARTICLE INFO

Article history:
Received 16 September 2015
Received in revised form
30 October 2015
Accepted 31 October 2015
Available online 18 December 2015

Key words:
Metal matrix composite
Shape memory alloy
Interface
Differential scanning calorimetry (DSC)
Damping

NiTi particles reinforced aluminum (NiTip/Al) composite was prepared via friction stir processing, eliminating interfacial reaction and/or elemental diffusion. The NiTip in the composite maintained the intrinsic characteristic of a reversible thermoelastic phase transformation even after heat-treatment. The shape memory characteristic of the NiTip decreased the coefficient of thermal expansion of the Al matrix, and an apparent two-way shape memory effect was observed in the composite. The composite owned a good combination of adjustable damping and thermal physical properties.

1. Introduction

Shape memory alloys (SMAs) such as NiTi have the ability to recover their original shape after being deformed, and this unique shape memory effect (SME) comes from a reversible thermoelastic phase transformation between a low-temperature martensite phase (B19' or R structure) and a high-temperature austenite phase (B2 structure)[1–3]. SMAs are found to have a wide application as smart materials because of such an SME[4,5].

By incorporating SMAs into polymer or metal matrices, the composites with special functions have been produced. Kirkby et al.[6] fabricated self-healing polymers with embedded NiTiCu SMA wires. The addition of SMA wires improved peak fracture loads, which approached the performance of the virgin material. Liu et al.[7] reported that the magnetic SMA particles (NiMnInCo) in a polyester matrix still maintain the magnetostructural transition behavior.

When fabricating the SMAs reinforced metal matrix composites (MMCs) using common cast and powder metallurgy (PM) processes, serious interfacial reaction and diffusion occurred between the SMAs and matrix alloys[8–10], decreasing the interfacial bonding strength due to the formation of brittle intermetallics[11,12], and degrading the SME due to the variation in the composition of the SMAs. Therefore, it is interesting and enlightening to fabricate an SMAs/Al composite without interfacial reactions and to understand the SME of the composite.

Friction stir processing (FSP) is a new processing technique, developed based on the basic principles of friction stir welding (FSW)[13]. An outstanding function of FSP is fabricating MMCs, especially those difficult to produce by conventional methods; however, so far research efforts are mainly focused on the fabrication of surface composites[14–17], and there are very few reports on how to obtain bulk composites[18,19].

Recently, Dixit et al.[20] fabricated a surface NiTi/1100Al composite by FSP. They reported that no interfacial reaction was detected, and the SME of NiTip could induce residual compressive and tensile stresses in the matrix, improving the mechanical properties of the composite. However, in order to achieve a wide application of the SMAs reinforced MMCs, it is necessary to fabricate the bulk composites and understand their physical properties associated with the SME.

In our previous study[21], bulk NiTip/6061Al composites were successfully fabricated by FSP using a special multi-hole particle presetting mode, which could help to homogeneously distribute the particles in the matrix. It was indicated that the composite exhibited tensile properties comparable to the 6061Al alloy. In the present study, the thermal physical properties and damping behavior of the composite were carefully examined. The aim is to understand the effect of NiTip addition on the physical properties of aluminum alloys.

* Corresponding author. Ph.D.; Tel.: +86 24 83978908; Fax: +86 24 83978908.
E-mail address: zyma@imr.ac.cn (Z.Y. Ma).

http://dx.doi.org/10.1016/j.jmst.2015.12.013

2. Experimental

Commercial 6061Al-T651 alloy plates of 6 mm thick and atomized $Ni_{49.5}Ti_{50.5}$ (at.%) particles with sizes of about 200 meshes were used in this study. The NiTip/6061Al composite was fabricated by FSP, and the detailed procedures have been described in our previous study[21]. To study the effect of heat-treatment on the SME of the composite, the as-FSP composite was subjected to aging (165 °C for 18 h, hereafter denoted as the FSP+aged composite) and T6 treatment (515 °C/40 min solutionized, 25 °C water quenched, 165 °C/18 h aged, hereafter denoted as the FSP+T6 composite), respectively. The microstructure of the as-FSP and FSP+T6 composites was examined by scanning electron microscopy (SEM), transmission electron microscopy (TEM), and high-resolution transmission electron microscopy (HRTEM).

Differential scanning calorimetry (DSC) testing was conducted on a DSC Q1000 V9.4 Build 287 machine at a heating rate of 10 °C min^{-1}. The as-FSP composite was subjected to cold-rolling treatment (kept in liquid nitrogen for 5 min, rolled along the FSP direction with a 5% reduction to investigate its effect on the physical properties. This step aims to induce the compressive residual stress in the matrix around the NiTip but almost does not change the microstructure of the composite). The rolled composite was machined into dimensions of 4 mm × 4 mm × 25 mm and subjected to a thermal expansion test on a NETZSCH DIL 409C machine, in a temperature range of –60 to 120 °C at a heating rate of 2 °C min^{-1}. For comparison, the as-FSP composite without rolling was also tested under the same condition.

Damping tests were carried out on a DMA machine (Model TA Q800) at the single cantilever vibration mode with dimensions of 30 mm × 3 mm × 1 mm. To measure strain-dependent damping capacities, samples were tested at room temperature at a vibration frequency of 1 Hz. For the measurements of temperature-dependent damping capacities, samples were tested at a strain amplitude of 1×10^{-4} in a temperature range of –80 to 90 °C at a heating/cooling rate of 3 °C min^{-1}, which is suitable for NiTi alloys based on previous studies[8,22].

3. Results and Discussion

3.1. Microstructure

The NiTip/6061Al composite fabricated in this study had a thickness of about 5 mm. The volume fraction of the NiTip in the composite was estimated to be about 10%. SEM examinations revealed that the NiTip were homogeneously distributed in the matrix (Fig. 1a), and the interface between the NiTip and Al matrix was clean without discernible reaction products (Fig. 1b). TEM examination further confirmed that no interfacial reactions occurred (Fig. 1c). This indicates that bulk aluminum matrix composite reinforced by homogeneously distributed NiTip was successfully fabricated without interfacial reaction.

The backscattered electron (BSE) image and EDS line scan analyses showed that no interfacial reaction or element diffusion occurred around the NiTip in the FSP+T6 composite (Fig. 1d). The TEM microstructure also showed that the interface was clean (Fig. 1e). The HRTEM analysis further revealed that no interfacial products but a diffusion layer with a few nanometers in thickness was detected between the NiTip and Al matrix (Fig. 1f). This shows that the composite could be subjected to a proper heat treatment.

It was reported that the NiTip easily reacted with Al element when processed at high temperatures, resulting in the generation of intermetallics at the NiTi–Al interface[9,10]. Thorat et al.[8] reported that for the NiTip/2124Al composite processed by the PM process, the interface reaction was obvious, with the NiTip surrounded by a layer of diffused interface products, Al_3Ti and Al_3Ni. Furthermore, Al atoms diffused into the NiTip to form an Al-rich layer, and this affected the transformation behavior by broadening the

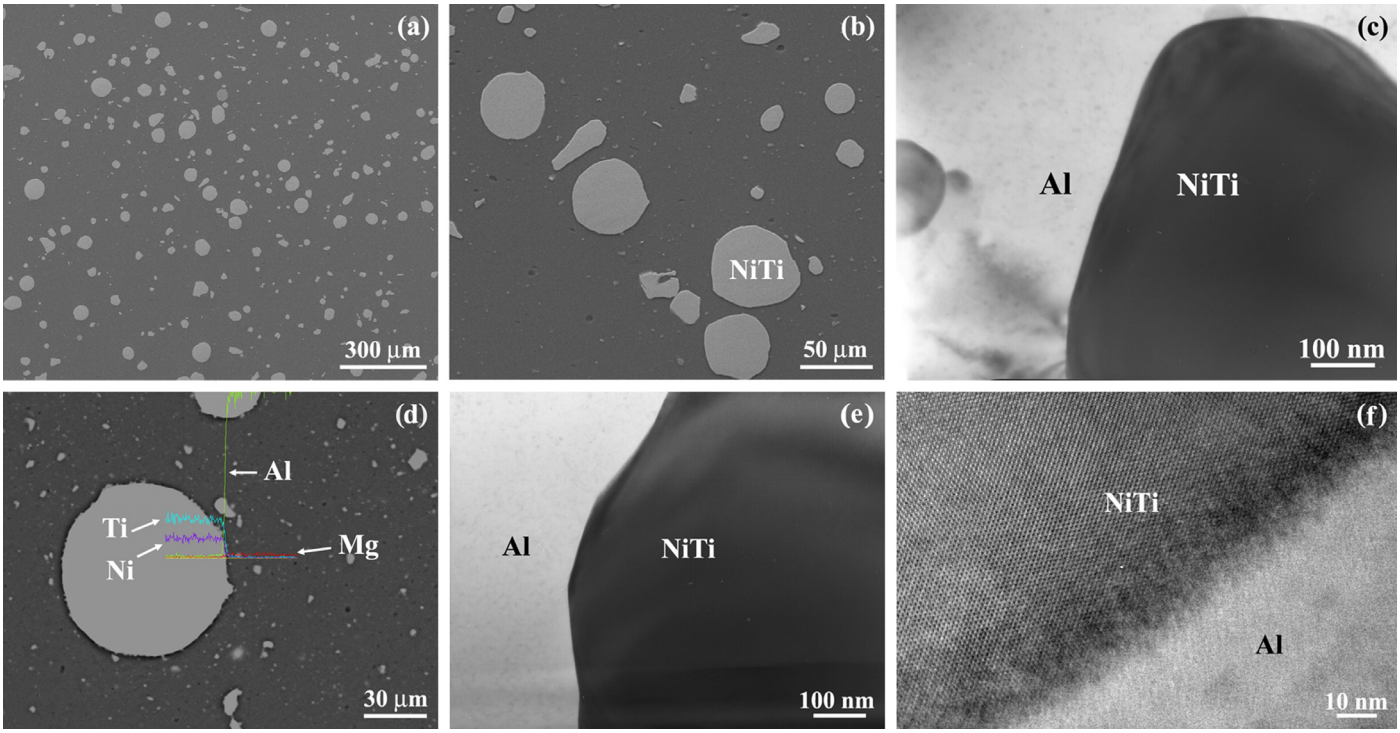

Fig. 1. SEM/TEM images of NiTip/6061Al composite under (a), (b), (c) as-FSP and (d), (e) (f) FSP+T6 conditions showing uniform distribution and clean interface of NiTip ((a), (b) SEM; (c), (e), (f) TEM; (d) backscattered electron image (BSE) with EDS).

intermediate R-phase transformation range. Although the interfacial reaction could be inhibited by shortening the sintering time[22], the considerably shorter sintering time and lower temperature are not beneficial to achieving high-quality composite billets. By contrast, the process temperature during FSP was much lower with significantly shorter duration[23], which effectively inhibited the interface reaction.

3.2. Shape memory effect

The DSC curves of the as-received NiTip exhibited a reversible phase transformation between martensite and austenite (Fig. 2a). In the cooling cycle of the as-received NiTip, three distinct peaks appeared, showing that the martensitic transformation occurred in three steps. For the NiTi alloys, a two-step martensitic transformation may usually occur[24,25]. The formation of the R-phase is favored during the cooling cycle due to the formation of fine and coherent Ni_4Ti_3 precipitates within the B2 microstructure, so the B2 transforms to the R-phase in the first step, and with further cooling the R-phase transforms to B19'. The multiple-steps transformation of the NiTi alloys has been widely reported and explained previously[24–28], and it was well established that these three peaks corresponded to the transformation of B2→R, R→B19', and B2→B19', respectively[24,26]. In the heating cycle, the phase transformation appeared in two steps: from the B19' to the B2 via the intermediate R-phase.

Compared to the as-received NiTip, two peaks appeared on both the cooling and heating cycle curves of the as-FSP, FSP+aged, and FSP+T6 composites (Fig. 2b–d), showing that the intrinsic phase transformation characteristic of the NiTip still remained. The peaks on the DSC curves of the as-FSP composite were much flatter than those of the as-received NiTip (Fig. 2b). The FSP+aged composite showed similar DSC curves to those of the as-FSP composite (Fig. 2c), indicating that the aging process had little effect on the phase transformation behavior. However, the DSC profiles of the FSP+T6 composite were quite different from those of the as-FSP composite (Fig. 2d): (1) the phase transformations were apparently promoted and the peaks on the curves were sharp; (2) the R transformation peak was greatly weakened and shifted toward higher temperatures during the heating cycle.

When the SMAs/Al composites were cooled down to room temperature from high temperature, residual thermal stress, normally compressive stress, was generated in the Al matrix due to the mismatch of the coefficient of thermal expansion (CTE) between the reinforcement and matrix, and this compressive stress is correlative to the reversible thermoelastic phase transformation[29]. Another possible reason is that the heat treatment may generate fine dispersed Ti_3Ni_4 precipitates in the B_2 phases, which are known to influence the phase transformation temperatures and to facilitate the R-phase transformation[27,28]; however, no precipitates were detected in the NiTip in the present study (Fig. 1e, f).

The addition of the NiTip effectively changed the CTE of the Al matrix (Fig. 3). The as-FSP composite showed an evidently negative CTE of about $-11 \times 10^{-6} K^{-1}$ within the temperature range of 14–18 °C during the heating cycle, which is significantly lower than that of the 6061Al (normally $23.6 \times 10^{-6} K^{-1}$), and it is about $22 \times 10^{-6} K^{-1}$ within the other temperature ranges, but it varied slightly during the cooling cycle.

It is seen that the as-FSP sample did not show SME. By contrast, the rolled composite showed a stronger CTE transformation behavior and a narrower transformation interval than the as-FSP

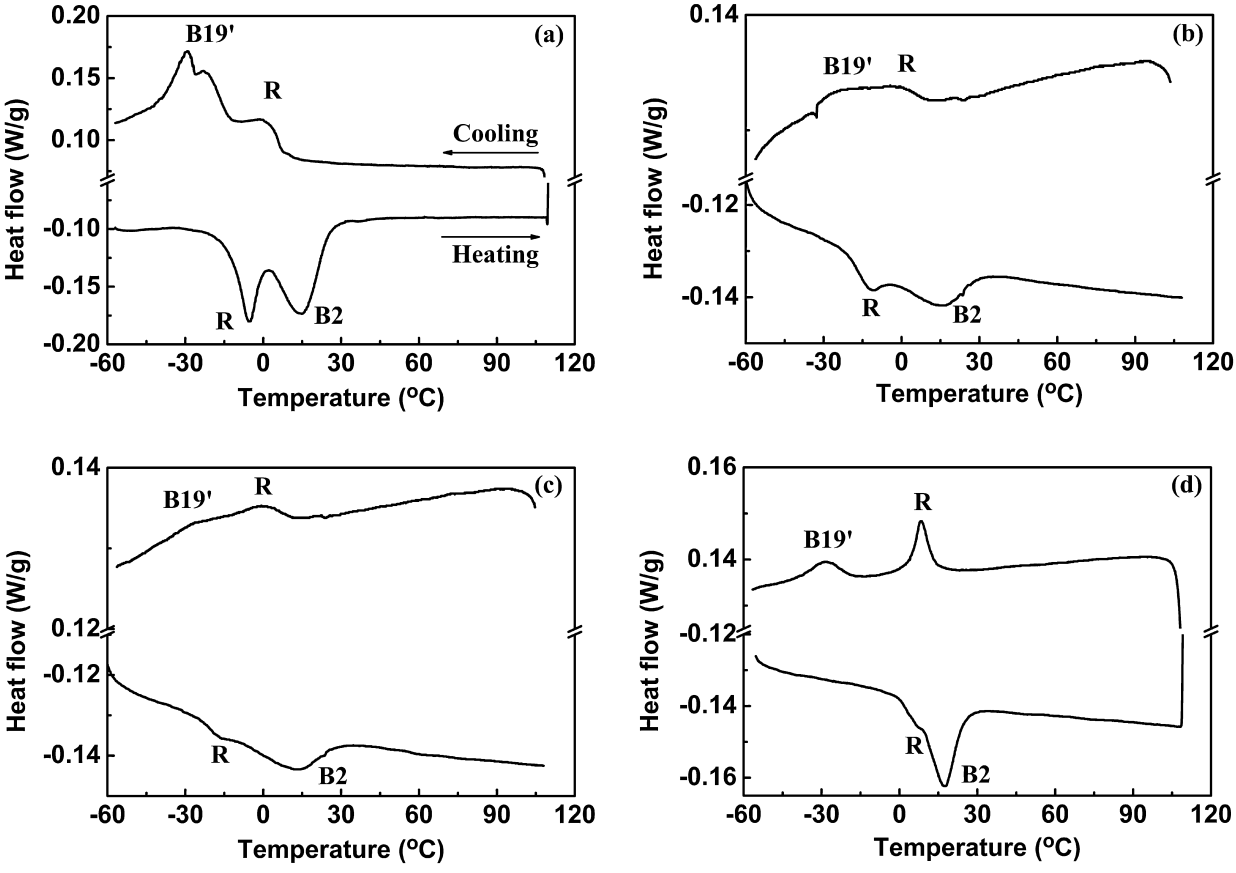

Fig. 2. DSC curves of (a) as-received NiTip, (b) as-FSP composite, (c) FSP+aged composite, and (d) FSP+T6 composite.

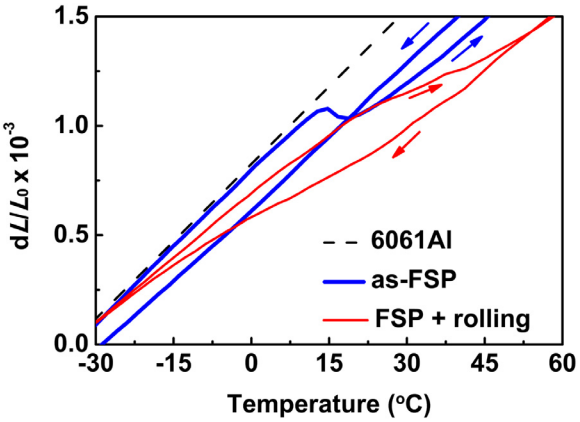

Fig. 3. Thermal expansion curves of NiTip/6061Al composites under as-FSP and rolled conditions.

counterpart. The different expansion behaviors between the as-FSP and rolled composites were because for the former the NiTip suffered isotropic thermoelastic martensitic transformation during the heating and cooling cycles, and for the latter the anisotropy of displacement appeared due to the directional stress-induced martensitic transformation.

The thermal expansion curves showed that the NiTip/6061Al composite retained the thermal expansion effect of the NiTip (Fig. 3), with controllable behaviors by cold working. The SME can be divided into one-way SME (OWSME) and two-way SME (TWSME)[30]. The OWSME is an intrinsic characteristic of SMAs, but the TWSME is an acquired characteristic that can be obtained by training[31]. It can be seen that the rolled FSP composite showed a clear TWSME.

3.3. Damping property

The strain dependent damping capacities of the NiTip/6061Al composites at room temperature are shown in Fig. 4a. All the composites showed slightly better damping capacities than the 6061Al, but almost no differences were observed among the damping capacities of the composites with different statuses. Fig. 4b shows the temperature-dependent damping capacities of the composites and 6061Al with corresponding storage modulus being shown in Fig. 4c. The 6061Al showed no damping peaks; however, owing to the presence of the NiTip, each of the composites owned an obvious heating/cooling loop (Fig. 4b). Furthermore, damping peaks which were accompanied by a shift in the storage modulus (Fig. 4c) were observed on both the heating and cooling loops of each composite due to the transformation behavior of the NiTip.

The storage modulus of both the composites and 6061Al decreased as the temperature increased (Fig. 4c). While the as-FSP composite showed similar storage moduli to the 6061Al, both the FSP+aged and FSP+T6 composites, especially the latter, exhibited much higher storage moduli than the 6061Al. Furthermore, a trough appeared on both the heating and cooling curves of each composite, which corresponded to the damping peaks on the curves of the damping capacities.

The improved damping properties of the NiTi/6061Al composite should result from the incorporation of NiTip with good damping

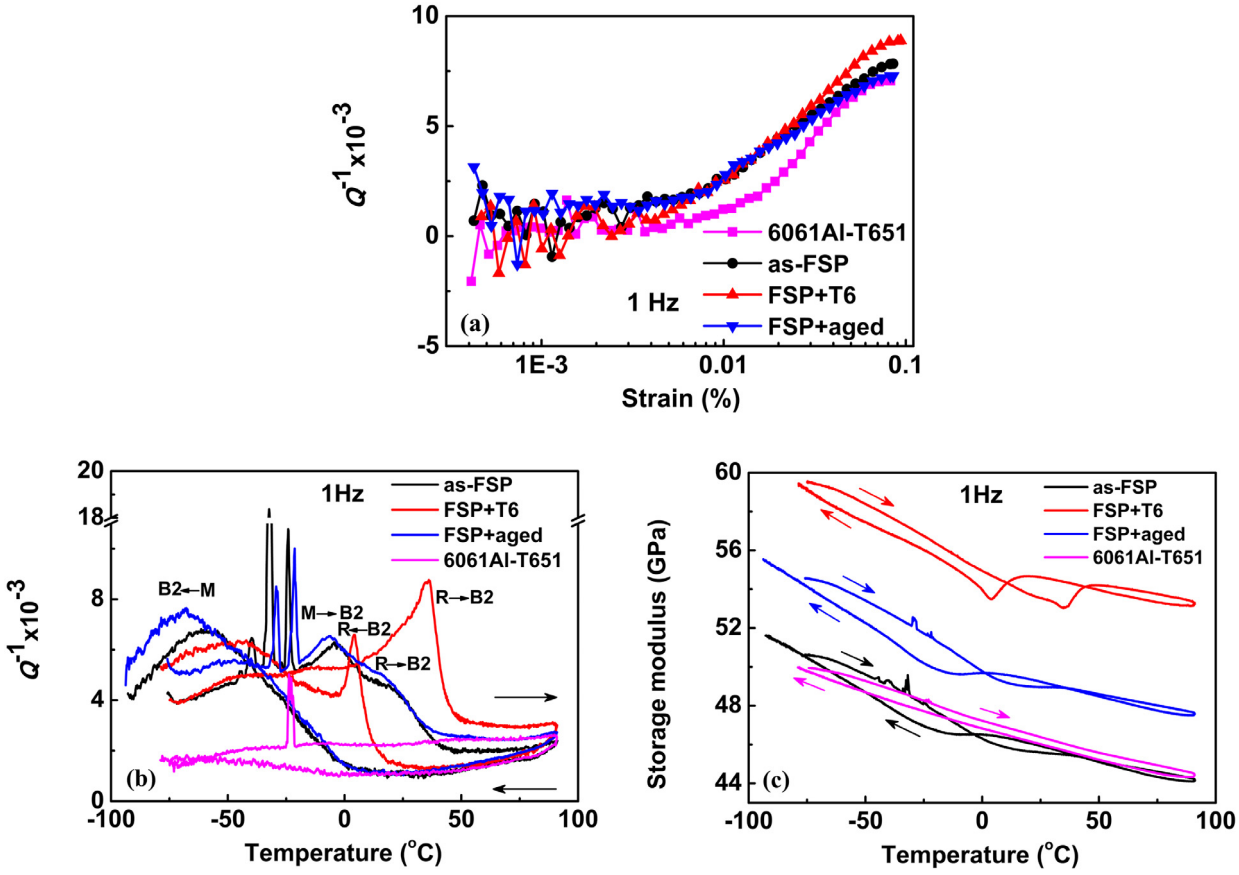

Fig. 4. (a) Strain-dependent damping capacities of NiTip/6061Al and 6061Al-T651 at room temperature, and (b) and (c) temperature-dependent damping capacities and storage modulus of NiTip/6061Al and 6061Al-T651.

properties (Fig. 4a–c). Zhang et al.[32] concluded that the damping properties of composites could be greatly improved by introducing high damping reinforcements. Meanwhile, this process could also introduce energy dissipation sources which are typically associated with the formation of crystallographic defects, such as fine and mobile grain boundaries, dislocations, and reinforcement/matrix interfaces. Furthermore, well-bonded interfaces may lead to an increased dislocation density near the interfaces through dislocation damping[32]. The FSP+T6 composite showed much sharper damping peaks compared to the other two composites, and this should also result from the generation of the compressive residual stress during the heat treatment as discussed above. It was noted that some extremely sharp peaks appeared on the curves at about –25 °C, and these peaks may result from the 6061Al itself but not the presence of the NiTip.

4. Conclusion

Bulk NiTip/6061Al composite with homogeneous particle distribution and without interface reaction products was successfully prepared by FSP. The composite retained the intrinsic characteristic of a reversible thermoelastic phase transformation of the NiTip and exhibited the shape memory characteristic which decreased the CTE. After cold rolling the composite showed an apparent TWSME. The composite could obtain a good combination of damping and thermal physical properties through a proper heat-treatment process.

Acknowledgments

This work was financially supported by the National Natural Science Foundation of China (Nos. 51101155 and 51331008) and the National Basic Research Program of China (No. 2012CB619600).

References

[1] M. Zarinejad, Y. Liu, Adv. Funct. Mater. 18 (2008) 2789–2794.
[2] W.Y. Ni, Y.T. Cheng, D.S. Grummon, Appl. Phys. Lett. 82 (2003) 2811–2813.
[3] Y.J. Zheng, L.S. Cui, J. Schrooten, Appl. Phys. Lett. 84 (2004) 31–33.
[4] L. Sun, W.M. Huang, Z. Ding, Y. Zhao, C.C. Wang, H. Purnawali, C. Tang, Mater. Des. 33 (2012) 577–640.
[5] J.M. Jani, M. Leary, A. Subic, M.A. Gibson, Mater. Des. 56 (2014) 1078–1113.
[6] E.L. Kirkby, J.D. Rule, V.L. Michaud, N.R. Sottos, S.R. White, J.A.E. Manson, Adv. Funct. Mater. 18 (2008) 2253–2260.
[7] J. Liu, N. Scheerbaum, S. Weiss, O. Gutfleisch, Appl. Phys. Lett. 95 (2009) 152503.
[8] R.R. Thorat, D.D. Risanti, D.S. Martín, G. Garcés, P.E.J. Rivera-Diaz-del-Castillo, S. van der Zwaag, J. Alloy Compd. 477 (2009) 307–315.
[9] G.A. Porter, P.K. Liaw, T.N. Tiegs, K.H. Wu, JOM (2000) 52–56.
[10] J.H. Lee, K. Hamada, K. Miziuuchi, M. Taya, K. Inoue, Mater. Res. Soc. Symp. 459 (1997) 419–424.
[11] K. Mizuuchi, JOM (2000) 26–31.
[12] Z.G. Wei, C.Y. Tang, W.B. Lee, J. Mater. Process. Technol. 69 (1997) 68–74.
[13] Z.Y. Ma, Metall. Mater. Trans. A 39 (2008) 642–658.
[14] R.S. Mishra, Z.Y. Ma, Mater. Sci. Eng. R 50 (2005) 1–78.
[15] H.B. Xu, C.R. Hubbard, K. An, Z.L. Feng, X.L. Wang, J. Qu, Adv. Eng. Mater. 11 (2009) 650–653.
[16] Y. Morisada, H. Fujii, T. Nagaoka, M. Fukusumi, Scr. Mater. 55 (2006) 1067–1070.
[17] L.B. Johannes, L.L. Yowell, E. Sosa, S. Arepalli, R.S. Mishra, Nanotechnology 17 (2006) 3081–3084.
[18] W. Wang, Q.Y. Shi, P. Liu, H.K. Li, T. Li, J. Mater. Process. Technol. 209 (2009) 2099–2103.
[19] K. Sun, Q.Y. Shi, Y.J. Sun, G.Q. Chen, Mater. Sci. Eng. A 547 (2012) 32–37.
[20] M. Dixit, J.W. Newkirk, R.S. Mishra, Scr. Mater. 56 (2007) 541–544.
[21] D.R. Ni, J.J. Wang, Z.N. Zhou, Z.Y. Ma, J. Alloy Compd. 586 (2014) 368–374.
[22] D. San Martín, D.D. Risanti, G. Garcés, P.E.J. Rivera-Diaz-del-Castillo, S. van der Zwaag, Mater. Sci. Eng. A 526 (2009) 250–252.
[23] Y.S. Sato, M. Urata, H. Kokawa, Metall. Mater. Trans. A 33 (2002) 625–635.
[24] K. Otsuka, X. Ren, Prog. Mater. Sci. 50 (2005) 511–678.
[25] J.I. Kim, Y.N. Liu, S. Miyazaki, Acta Mater. 52 (2004) 487–499.
[26] N. Resnina, S. Belyaev, J. Alloy Compd. 486 (2009) 304–308.
[27] J. Khalil Allafi, A. Dlouhy, G. Eggeler, Acta Mater. 50 (2002) 4255–4274.
[28] J. Khalil Allafi, X. Ren, G. Eggeler, Acta Mater. 50 (2002) 793–803.
[29] D.R. Ni, Z.Y. Ma, Acta Metall. Sin. (Eng. Lett.) 27 (2014) 739–761.
[30] Y. Freed, J. Aboudi, Int. J. Solids Struct. 46 (2009) 1634–1647.
[31] W. Huang, Mater. Des. 23 (2002) 11–19.
[32] J.M. Zhang, R.J. Perez, C.R. Wong, E.J. Lavernia, Mater. Sci. Eng. R 13 (1994) 325–389.